https://doi.org/10.1016/j.apacoust.2018.08.023

Technical Note

Hybrid noise control using multiple Helmholtz resonator arrays

Dizi Wu[1], Nan Zhang[2] , Cheuk Ming Mak[3] and Chenzhi Cai[1,3, *]

[1]*School of Civil Engineering, Central South University, Changsha, Hunan, China;*

[2]*School of Architecture and Art, Central South University, Changsha, Hunan, China;*

[3]*Department of Building Services Engineering, The Hong Kong Polytechnic University, Hung Hom, Kowloon, Hong Kong, China*

*Corresponding author.
E-mail Address: chenzhi.cai@connet.polyu.hk (C.Cai)
Telephone: +852 2766 4049

Abstract

Helmholtz resonator (HR) is one of the most basic acoustic models and is generally used to reduce low-frequency noise. However, it is only effective at its single resonance peak with narrow frequency band. In order to deal with low-frequency, broadband and hybrid noise in a ventilation ductwork system, a multiple HR arrays system is therefore proposed in this paper. Several tuned HRs mounted on the same cross-sectional area of the duct is considered as a transverse HR array. By distributing the transverse HR array periodically along the duct, the multiple HR arrays system is then proposed to eliminate hybrid noise in a ventilation ductwork system. The acoustic performance of the proposed multiple HR arrays system is analyzed theoretically and numerically. The transfer matrix method and the Bragg theory are used to investigate wave propagation through the duct. Owing to the coupling effects of the Bragg refection and HRs' resonances, several broadband noise attenuation bands can be obtained. The theoretical predictions show good agreement with the three-dimensional Finite Element Method (FEM) simulation results. The present study provides a practical way in hybrid noise control application of the ventilation ductwork system and other research areas in respect of the HR.

Keywords: Helmholtz resonator; hybrid noise; transmission loss; multiple; finite element method

1. Introduction

The ventilation ductwork system is almost indispensable in modern buildings, especially in hot and humid regions that provides a thermally comfortable indoor environment as well as good indoor air quality [1]. However, as the ventilation ductwork system begins to operate, the undesired flow-generated noise due to the discontinuity of the duct will come along with the fresh and thermal comfortable air [2-4]. People spend nearly 87% of their times indoors which includes an eight-hour daily for a five-day workweek in office [5,6]. Therefore, there has been a growing concern about indoor noise in recent years, since noise has significant impacts on people’s comfort, health and productivity. Long-term noise exposure would bring the negative impacts on people’s physiological and psychological conditions even through within the limit of allowable noise level [7-9]. Noise exposure is relevant to some negative symptoms and cardiovascular disease, for instance sleeping problem, headache, tinnitus, heart disease and myocardial infarction [10-15]. The accompanied noise with air from the ventilation ductwork system is the main source that deteriorates the indoor acoustic environment. Therefore, the noise attenuation performance technologies for the ventilation ductwork system have received extensive worldwide attentions recently, especially the low-frequency and broadband noise.

Generally, there are two types of noise control methods for ventilation ductwork system: active noise control and passive noise control. Although active noise control system has the potential advantage of controlling low-frequency, there are problems related to its reliability and high cost [16,17]. The traditional passive noise control (the dissipative silencer and the reactive silencer) still suffer from some obvious drawbacks. The dissipative silencer can absorb noise from mid to high frequencies effectively, however, it can hardly reduce any noise at low frequencies. Bedsides, porous sound absorption materials used in the dissipative silencer are good matrix for bacterial breeding and accumulation of dusts [18]. The reactive silencer, for instance the Helmholtz resonator and expansion chamber, shows stabilized noise control performance and can be affordable. The effective noise control range of the reactive silence can be tuned conveniently because it is only depended on the geometries of the reactive silence [19-22]. Nevertheless, the volume of the expansion chamber needs to be enormous in order to reduce low-frequency noise in a ventilation ductwork system and it seems to be impractical in engineering applications [20]. The Helmholtz resonator (HR) presents a solution for low frequencies noise control, however, it is only useful against noise centralized in a very narrow frequency band and it is unable to deal with hybrid noise.

Over the years, a number of investigators have tried to improve the acoustic performance of a HR and to devise a method for broadband noise attenuation band at low frequencies. Various modified HRs have been proposed and examined, for instance HR with spiral neck, HR with extended neck [23], dual HR formed by a pair of neck and cavity [24], parallel-coupled HR through a thin membrane [25] and micro-perforated absorbers backed by HR [26]. However, these modified HRs are still qualified as narrow-band silencer. It is therefore that a lot of efforts have been made to broaden the noise attenuation bands. Combing several different Helmholtz resonators is a possible way, which means using serial or parallel arrangement of Helmholtz resonators with different resonance frequencies to obtain a wide band of noise control in ducts [27-29]. However, these HRs should be tuned carefully and will occupy a large space. By introducing the coupling effects of Bragg reflection and HR's resonance, a periodic HR array can provide a much broader noise attenuation bands at the HR's resonance frequency. The propagation of time harmonic acoustic wave in periodic waveguides had been investigated theoretically and experimentally [30,31]. The peculiar dispersion characteristics of waves propagation through a tunnel mounted with identical HRs periodically had been revealed, labelled as stopbands and passbands [32]. However, the attenuation bandwidth of a periodic ducted HR system compromises the peak amplitude [33]. Moreover, a periodic ducted HR system cannot cope with hybrid noise which commonly exists in practical ventilation ductwork system.

In order to deal with low-frequency, broadband and hybrid noise in a ventilation ductwork system, a multiple HR arrays system is therefore proposed in this paper. Several tuned HRs mounted on the same cross-sectional of the duct is considered as a transverse array. The transverse HR array distributed periodically along the longitudinal direction of the duct is then introduced as the multiple HR arrays system. In light of low frequencies considered in this paper are well below the duct's cutoff frequency, only planar wave is assumed to propagate through the duct. The Bragg theory and the transfer matrix method are used to conduct the investigation. The acoustic performance of the proposed multiple HR arrays system is analyzed theoretically and numerically. The transverse HR array could provide several different resonance peaks. The periodic structure could provide broader noise attenuation bands due to the coupling effects of Bragg reflection and HRs' resonances. It is therefore that several broadband noise attenuation bands at designed HRs' resonances can be achieved by using the multiple HR arrays system. The theoretical predictions are validated by the three-dimensional Finite Element Method (FEM) simulation. A good agreement between the theoretical predictions and FEM simulation results can be found. The present study provides a potential way to deal with commonly existed hybrid noise in ventilation ductwork system and other research areas in respect of the HR.

2. Theoretical analysis of a transverse Helmholtz resonator array

2.1 A single side-branch Helmholtz resonator

The classical approach in modelling a HR as an equivalent spring-mass system with end-correction length to account for the multidimensional wave effects. To improve the accuracy of the predictions, wave propagation approach developed from one-dimensional approach to multidimensional approach. Indeed, the sound fields inside an HR are clearly multidimensional because of sudden discontinuity interface. The multidimensional wave propagation approach can provide a more accurate prediction [22]. However, in light of low frequencies of interest in the ventilation ductwork system, wavelengths of considered frequencies in this paper are significant larger than the dimensions of the HR. Moreover, the main purpose of this paper is to investigate the acoustic performance of the multiple HRs arrays system for hybrid noise control. Therefore, the classical approach with end-correction length is adopted here and the acoustic impedance of a HR is given as [19]:

$$Z_r = j(\omega \frac{\rho_0 l_n'}{S_n} - \frac{1}{\omega} \frac{\rho_0 {c_0}^2}{V_c}) \tag{1}$$

where Z_r represents the acoustic impedance of the HR, ρ_0 and c_0 are air density and speed of sound in the air respectively, l_n' and S_n are the neck's effective length and area respectively, V_c is the cavity volume, ω is the circular frequency.

Figure 1 illustrates the schematic diagram of a single side-branch HR mounted on the duct with cross-section area S_d . Once the acoustic impedance of the HR has been obtained according to Eq. (1), the transmission loss of the single side-branch HR can be determined by the four-pole parameter method as [34]:

$$TL = 20\log_{10}\left(\frac{1}{2}\left|2+\frac{\rho_0 c_0}{S_d}\frac{1}{Z_r}\right|\right) \tag{2}$$

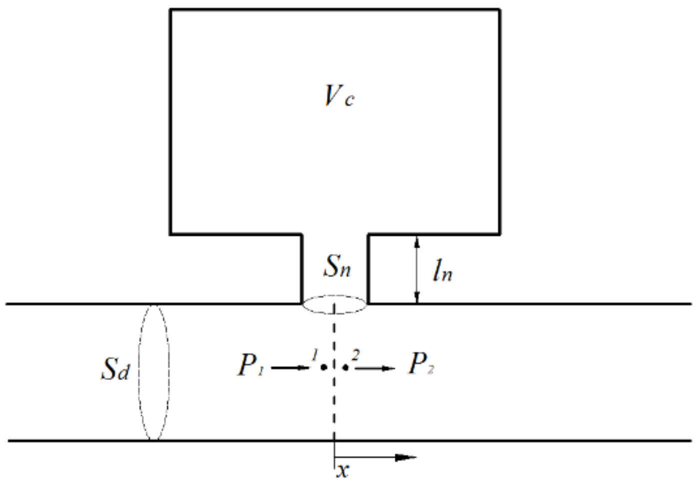

Figure 1. A single side-branch Helmholtz resonator

2.2 A single side-branch Helmholtz resonator

It is well known that the HR is only effective against noise centralized in a very narrow frequency band and it is unable to deal with hybrid noise. Several HRs with different resonance frequencies mounted on the same cross-sectional of the duct is a possible way for hybrid noise control. The transverse HR array with N (N=4 here for example) different HRs mounted on the same cross-section of the duct is illustrated in Figure 2. On the basis of low frequencies considered in this paper, only planar wave is assumed to propagate through the main duct. Taking no account of the time-harmonic disturbance and the reflected waves from downstream of the duct, the sound pressures and the particle velocities illustrated in Figure 2(a) can be expressed as:

$$p_1(x) = I_1 e^{-jkx} + R_1 e^{jkx}, \quad p_2(x) = I_2 e^{-jkx} \tag{3}$$

$$u_1(x) = \frac{I_1}{S_d Z_d} e^{-jkx} - \frac{R_1}{S_d Z_d} e^{jkx},\; u_2(x) = \frac{I_2}{S_d Z_d} e^{-jkx} \tag{4}$$

where k is the wave number, Z_d is the acoustic impedance of the duct, S_d is the cross-sectional area of the duct, I_i and R_i (i=1,2) represent respective complex wave amplitudes.

The acoustic impedances of these different HRs mounted on the same cross-sectional area of the duct can be calculated by Eq. (1), expressed as Z_{r1}, Z_{r2}, Z_{r3} and Z_{r4} respectively. As depicted in Figure 2(b), the continuity conditions of sound pressure and volume velocity at the duct-neck interface yield:

$$p_1 = p_2 = p_{f1} = p_{f2} = p_{f3} = p_{f4} \tag{5}$$

$$S_d u_1 = S_d u_2 + \frac{p_{f1}}{Z_{r1}} + \frac{p_{f2}}{Z_{r2}} + \frac{p_{f3}}{Z_{r3}} + \frac{p_{f4}}{Z_{r4}} \tag{6}$$

Combining Eq. (5) and Eq. (6), the relation between point 1 to point 2 could be expressed in the following matrix form as:

$$\begin{bmatrix} p_1 \\ \rho_0 c_0 u_1 \end{bmatrix} = \begin{pmatrix} 1 & 0 \\ \frac{\rho_0 c_0}{S_d}\left(\frac{1}{Z_{r1}} + \frac{1}{Z_{r2}} + \frac{1}{Z_{r3}} + \frac{1}{Z_{r4}}\right) & 1 \end{pmatrix} \begin{bmatrix} p_2 \\ \rho_0 c_0 u_2 \end{bmatrix} \tag{7}$$

Then, the transmission loss of the transverse HR array can be obtained as:

$$TL = 20\log_{10}\left(\frac{1}{2}\left|2 + \frac{\rho_0 c_0}{S_d}\left(\frac{1}{Z_{r1}} + \frac{1}{Z_{r2}} + \frac{1}{Z_{r3}} + \frac{1}{Z_{r4}}\right)\right|\right) \tag{8}$$

It can be observed from Eq. (8) that the resonance frequencies of the transverse HR array still depend on the resonance frequency of each individual HR. The resonance frequency of a HR is only determined by its geometries. It indicates that it is easy to obtain a transverse HR array with desired resonance frequencies for hybrid noise control at low frequencies.

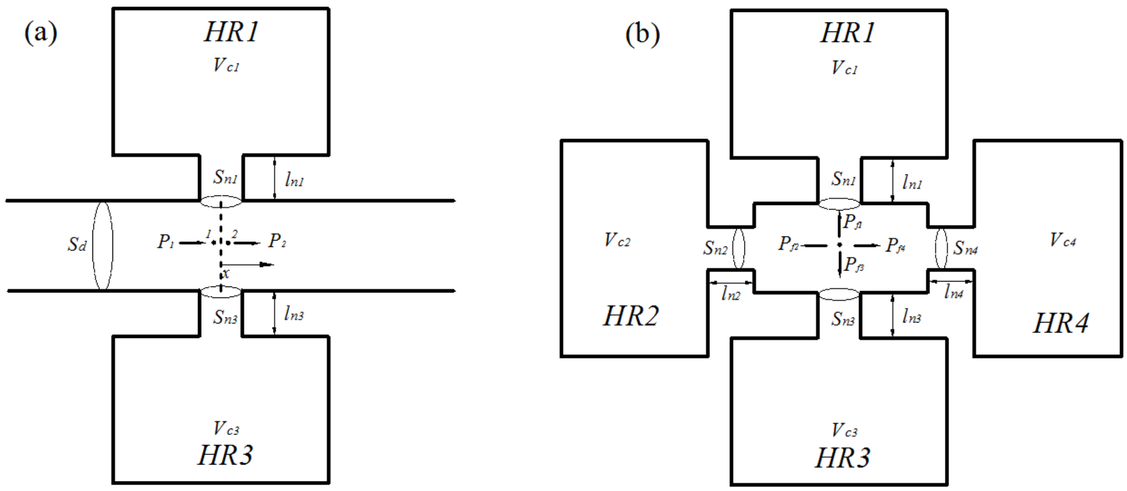

Figure 2. A transverse HR array consisting of four different HRs (a) side view, (b) front view

3. Wave propagation in a duct with a multiple Helmholtz resonator arrays system

Although the aforementioned transverse HR array could provide several attenuation bands at its designed resonance frequencies, the narrow-band behavior of the transverse HR array is not practical to be used in engineering applications. In order to deal with low-frequency, broadband and hybrid noise in a ventilation ductwork system, an array of transverse HRs array distributed periodically on the duct, as shown in Figure 3, is proposed to be the multiple HR arrays system. The periodicity of the multiple HR arrays system can broaden the noise attenuation bands at the resonance frequencies of the transverse HR array. A periodic unit is composed of a duct segment and a transverse HR array. By assuming the neck diameters of all HRs are negligible compared with the length of duct segment in a periodic cell, it is therefore that the duct segment's length is regarded as the periodic distance. In light of low frequencies is the main concern in ventilation ductwork system noise control, the frequencies considered in this paper is well below the duct's cutoff frequency. Therefore, only planar wave is assumed to propagate through the duct. The characteristics of sound wave in the *nth* unit could be described as sound pressure $p_n(x)$ and particle velocity $u_n(x)$.Assuming a time-harmonic disturbance in the form of $e^{j\omega t}$, both the sound pressure and particle velocity can be expressed by the combination of the positive-*x* and negative-*x* directions as:

$$p_n(x) = I_n e^{-jk(x-x_n-\omega t)} + R_n e^{jk(x-x_n+\omega t)} \tag{9}$$

$$u_n(x) = \frac{I_n}{\rho_0 c_0} e^{-jk(x-x_n-\omega t)} - \frac{R_n}{\rho_0 c_0} e^{jk(x-x_n+\omega t)} \tag{10}$$

where *k* is the number of waves, $x_n = (n-1)d$ represents the local coordinates, d is the periodic distance, and I_n and R_n represent respective complex wave amplitudes. According to Eq. (8), the transverse HR array could be considered as 'an equivalent HR' with equivalent acoustic impedance of $Z_e = Z_{r1}Z_{r2}Z_{r3}Z_{r4} / (Z_{r1}Z_{r2}Z_{r3} + Z_{r1}Z_{r2}Z_{r4} + Z_{r1}Z_{r3}Z_{r4} + Z_{r2}Z_{r3}Z_{r4})$ in the multiple HR arrays system. Considering the continuity conditions of sound pressure and volume velocity at the point *x*=*nd* yield:

$$\begin{bmatrix} I_{n+1} \\ R_{n+1} \end{bmatrix} = \begin{bmatrix} \exp(-jkd) & 0 \\ 0 & \exp(jkd) \end{bmatrix} \begin{bmatrix} (1-\rho_0 c_0/2S_d Z_e) & -\rho_0 c_0/2S_d Z_e \\ \rho_0 c_0/2S_d Z_e & (1+\rho_0 c_0/2S_d Z_e) \end{bmatrix} \begin{bmatrix} I_n \\ R_n \end{bmatrix} = \mathbf{T} \begin{bmatrix} I_n \\ R_n \end{bmatrix} \tag{11}$$

$\mathbf{T}$ is the transfer matrix. Once the initial sound pressure is given, the sound pressures and the particle velocities in arbitrary periodic unit could be obtained by Eq. (11). According to the Bloch wave theory, Eq. (11) can be expresses as [30]:

$$\begin{bmatrix} I_{n+1} \\ R_{n+1} \end{bmatrix} = \exp(-jqd) \begin{bmatrix} I_n \\ R_n \end{bmatrix} = \mathbf{T} \begin{bmatrix} I_n \\ R_n \end{bmatrix} \tag{12}$$

where q is the Bloch wave number. The transfer matrix can be set as $\mathbf{T} = \lambda$ (λ is set to be $\exp(-jqd)$). Therefore, the analysis of the multiple HR array system boils down to the solution of an eigenvalue and its corresponding eigenvector. The Bloch wave number q is allowed to be a complex value and may include a real part and an imaginary part. In general, there are two solutions for λ : λ_1 and λ_2 with corresponding eigenvectors $[v_{I1}, v_{R1}]^{\mathbf{T}}$ and $[v_{I2}, v_{R2}]^{\mathbf{T}}$ respectively. Then Eq. (12) can be rewritten as:

$$\begin{bmatrix} I_{n+1} \\ R_{n+1} \end{bmatrix} = \mathbf{T} \begin{bmatrix} I_n \\ R_n \end{bmatrix} = \mathbf{T}^2 \begin{bmatrix} I_{n-1} \\ R_{n-1} \end{bmatrix} = \ldots = \mathbf{T}^n \begin{bmatrix} I_1 \\ R_1 \end{bmatrix} = A_0 \lambda_1^n \begin{bmatrix} v_{I1} \\ v_{R1} \end{bmatrix} + B_0 \lambda_2^n \begin{bmatrix} v_{I2} \\ v_{R2} \end{bmatrix} \tag{13}$$

where λ_1 and λ_2 are assumed to describe the sound wave propagation through the positive-*x* and negative-*x* respectively. The boundary conditions determine the complex constants A_0 and B_0. The termination with reflection coefficient α yields:

$$\frac{R_n e^{jk(x - x_n + \omega t)}}{I_n e^{-jk(x - x_n - \omega t)}} = \frac{A_0 \lambda_1^{\,n-1} v_{R1} e^{jkL_{end}} + B_0 \lambda_1^{\,n-1} v_{R2} e^{jkL_{end}}}{A_0 \lambda_1^{\,n-1} v_{I1} e^{-jkL_{end}} + B_0 \lambda_1^{\,n-1} v_{I2} e^{-jkL_{end}}} = \alpha \tag{14}$$

The initial condition with given sound pressure yields:

$$\begin{aligned} p_0 &= I_0 e^{-jk(x+d)} + R_0 e^{jk(x+d)} \Big|_{x=-L_{start}} \\ &= (A_0 \lambda_1^{-1} v_{I1} + B_0 \lambda_2^{-1} v_{I2}) e^{-jk(d - L_{start})} + (A_0 \lambda_1^{-1} v_{R1} + B_0 \lambda_2^{-1} v_{R2}) e^{jk(d - L_{start})} \end{aligned} \tag{15}$$

Therefore, the transmission loss of the multiple HR arrays system could be expressed as:

$$TL = 20 \log_{10} \left| \frac{I_0}{I_{n+1}} \right| = 20 \log_{10} \left| \frac{A_0 \lambda_1^{-1} v_{I1} + B_0 \lambda_2^{-1} v_{I2}}{A_0 \lambda_1^{n} v_{I1} + B_0 \lambda_2^{n} v_{I2}} \right| \tag{16}$$

Assuming the duct ends with an anechoic termination ($\alpha = 0$), no reflected sound wave exists in the last part of the duct. According to Eq. (14), it can be seen that $B_0 = 0$ is mandatory under the assumed anechoic termination. Then, Eq. (16) can be simplified as

$TL = -20(n+1)\log_{10}|\lambda_1|$. The eigenvalue λ_1 is related to the frequency, periodic distance and the equivalent acoustic impedance of the transverse HR array, as indicated by Eq. (11).

Owing to the periodicity, the multiple HR arrays system can obtain broader noise attenuation bands at the designed resonance frequencies. Generally, there are two mechanism of noise attenuation bands: the resonances of HRs and the Bragg reflection. When the Bragg reflection is intended to occur at the resonance frequencies of HRs, the coupling effects of the Bragg reflection and HRs' resonances lead to broader noise attenuation bands. For a periodic structure, the Bragg reflection will exit near $f_m = mc_0 / 2d$ (m is integer) [32]. For a duct with periodic distributed identical HR (each periodic unit includes a single HR), the periodic distance is chosen to be $d = m\lambda_0/2$ (λ_0 is the resonance wavelength of the HR) for the coupling effects of HR's resonance and Bragg reflection. For the multiple HR arrays system, the transverse HR array can be considered as an 'equivalent HR' with equivalent acoustic impedance $Z_e = Z_{r1}Z_{r2}Z_{r3}Z_{r4} / (Z_{r1}Z_{r2}Z_{r3} + Z_{r1}Z_{r2}Z_{r4} + Z_{r1}Z_{r3}Z_{r4} + Z_{r2}Z_{r3}Z_{r4})$. It indicates that the 'equivalent HR' has four resonance frequencies as f_1, f_2, f_3 and f_4 (assuming $f_1 < f_2 < f_3 < f_4$). The corresponding wavelengths of these four resonance frequencies are λ_{01} , λ_{02} , λ_{03} and λ_{04} , with relationship of $\lambda_{01} > \lambda_{02} > \lambda_{03} > \lambda_{04}$. In order to obtain broader noise at every resonance frequency for hybrid noise control, the Bragg reflection frequencies need to coincide with resonance frequencies of the transverse HR array. It is therefore that the periodic distance d of the multiple HR arrays system needs to satisfy the following requirement:

$$d = m_1\lambda_{01}/2 = m_2\lambda_{02}/2 = m_3\lambda_{03}/2 = m_4\lambda_{04}/2 \qquad (17)$$

where m_i with subscript should be integral. As the integer number increases, the noise attenuation bands will decrease due to the reduced coupling effects of the Bragg reflection and HR's resonance [32]. For the sake of broader noise attenuation bands at each resonance frequencies simultaneously, the periodic distance is chosen as $d = \lambda_{01}/2 = \lambda_{02}/2 = 1.5\lambda_{03} = 2\lambda_{04}$. By tuning the resonance frequencies of the transverse HR array and choosing an appropriate periodic distance, the multiple HR arrays system can provide several broadband noise attenuation bands.

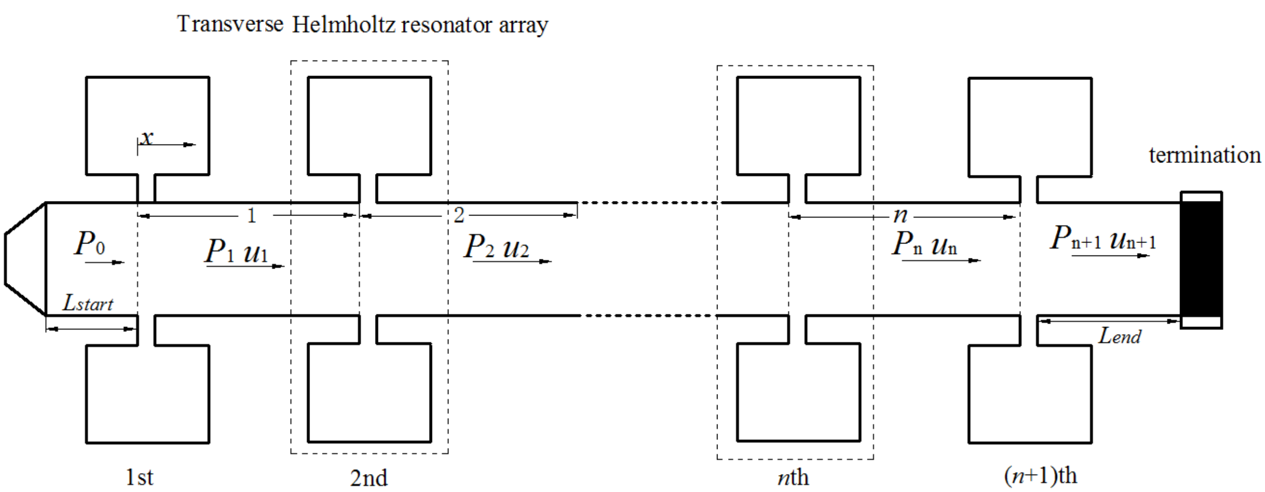

Figure 3. Multiple Helmholtz resonator arrays installed on the duct

4. Results and discussion

4.1 Validation of the theoretical predictions of a transverse HR array

The transverse HR array consists of four HRs are illustrated in Figure 2. The geometries of necks are: neck cross-sectional area $S_{n1} = S_{n2} = S_{n3} = S_{n4} = \pi \text{cm}^2$ and necks' length $l_{n1} = l_{n2} = l_{n3} = l_{n4} = 2.5\text{cm}$. The cavity volumes of HR1, HR2, HR3 and HR4 are: $V_{c1} = 753.7\pi \text{cm}^3$, $V_{c2} = 200\pi \text{cm}^3$, $V_{c3} = 89.6\pi \text{cm}^3$ and $V_{c4} = 51.5\pi \text{cm}^3$ respectively. The cross-sectional area of the main duct is $S_d = 64\text{cm}^2$. The resonance frequency of a HR is only determined by its geometries. It is therefore that the resonance frequencies of HR1, HR2, HR3 and HR4 are: 100Hz, 200Hz, 300Hz and 400Hz respectively. Figure 4 demonstrates the configurations of the transverse HR array model. The predicted transmission loss of the transverse HR array is compared with the transmission loss of these four individual HRs mounted on the duct independently, as shown in Figure 5. It can be observed from Figure 5 that the transverse HR array has four resonance frequencies with nearly the same peak amplitudes and bandwidths corresponding to each HR. The acoustic performance of the transverse HR array could be considered as the combination of these HRs' attenuation performances. Figure 6 shows a good agreement between the theoretical predictions and the three-dimensional FEM simulation results.

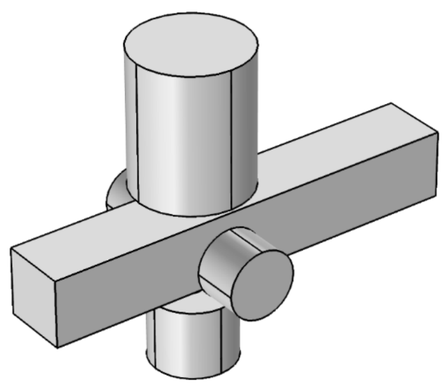

Figure 4. Configuration of a transverse HR array consisting of four different HRs

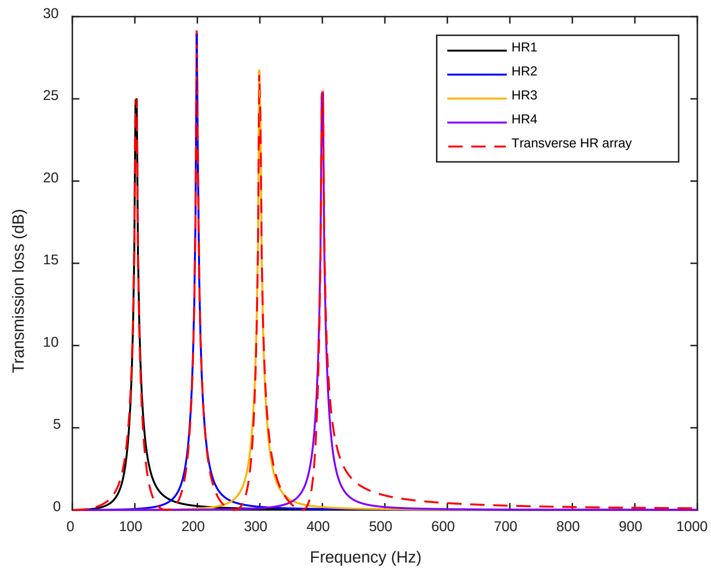

Figure 5. Comparison of the transverse HR array and individual HRs

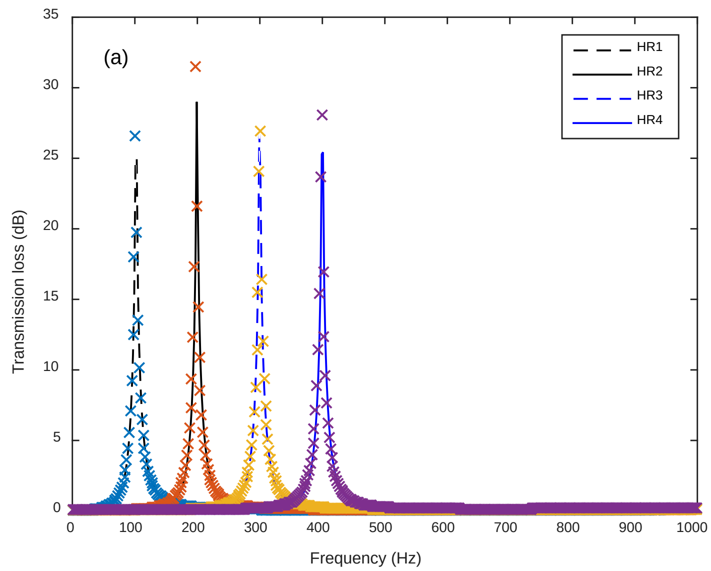

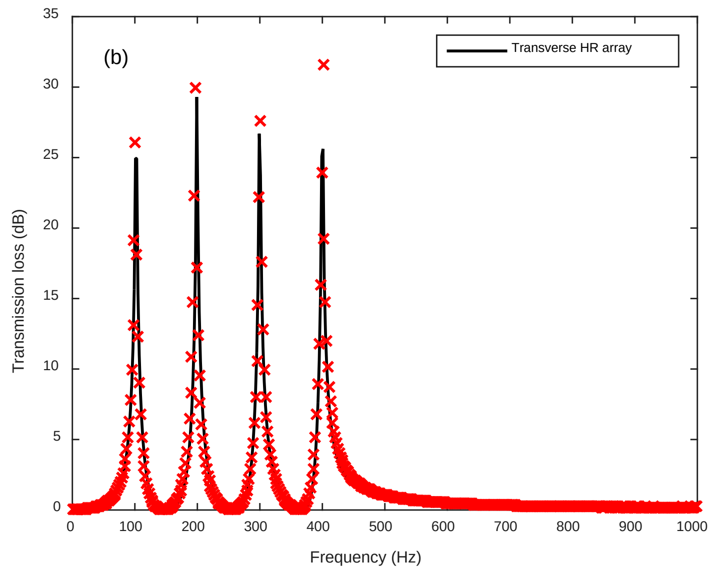

Figure 6. Comparison of theoretical predictions and the FEM simulation results (solid lines represent theoretical predictions, and dashed crosses represent the FEM simulation results)

4.2 Validation of the theoretical predictions of multiple HR arrays

The geometries of the transverse HR array and the main duct adopted here are the same as given above. The aforementioned transverse HR array can provide four different resonance frequencies corresponding to each HR's acoustic characteristics. However, the transverse HR array is still only effective at its resonances with relative narrow attenuation bands. By taking the advantage of the coupling effects of Bragg reflection and resonances of the transverse HR array, the periodic structure could provide broader noise attenuation bands at designed resonance frequencies. An array of transverse HRs array distributed periodically on the duct, as shown in Figure 3, is proposed to be the multiple HR arrays system. The end of the duct is set to be anechoic termination to avoid the reflected sound wave. An oscillating sound pressure at a magnitude of $P_0 = 1$ is applied at the beginning of the duct as the initial boundary condition. The configuration of the proposed multiple HR array systems consisting of five transverse HR arrays distributed periodically on the longitudinal direction of the duct is demonstrated in Figure 6. The resonance frequencies of HR1, HR2, HR3 and HR4 are designed to be 100Hz, 200Hz, 300Hz and 400Hz respectively. Thus, the designed resonance wavelengths of these HRs are designed to satisfy the requirement of $d = \lambda_{01}/2 = \lambda_{02}/2 = 1.5\lambda_{03} = 2\lambda_{04}$ for broader noise attenuation bands. Therefore, the Bragg reflection can coincide with these four resonance frequencies simultaneously. Figure 8 compares the transmission loss of the transverse HR array and transverse HR array as a periodic portion of the multiple HR array system. It can be seen from Figure 8 that four broader noise attenuation bands at the designed resonance frequencies can be achieved. The theoretical predictions fit well with the three-dimensional FEM simulation results, as illustrated in Figure 9.

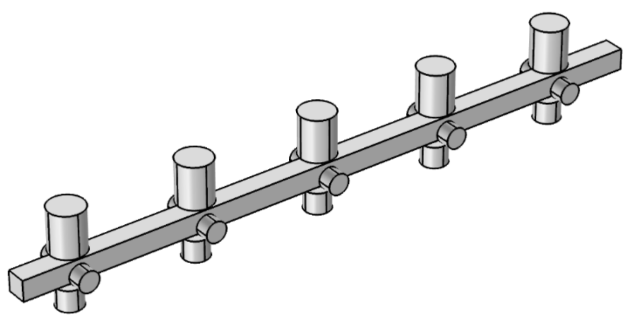

Figure 7. Configuration of the multiple HR arrays system

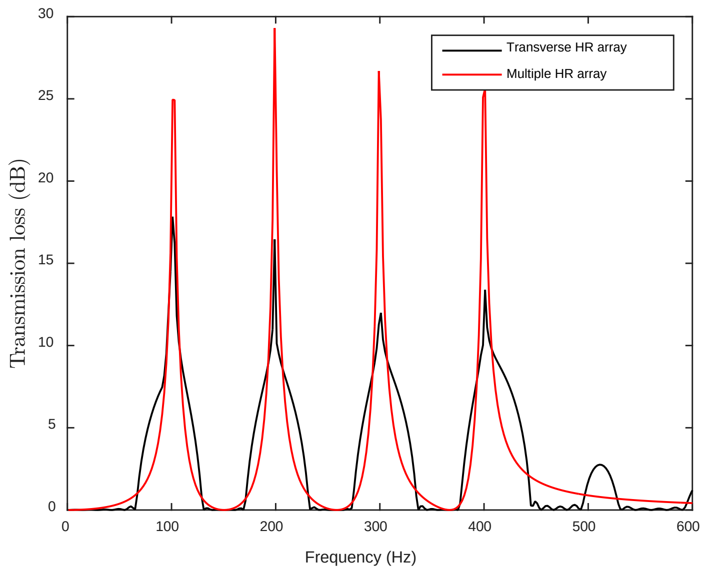

Figure 8. Comparison of the side-branch transverse HR array and the transverse HR array as a periodic portion of the multiple HR array system

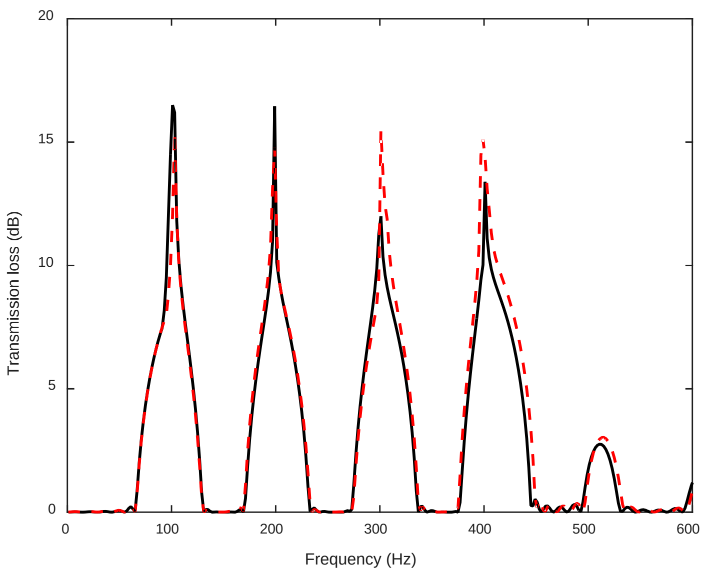

Figure 9. Comparison of theoretical predictions and the FEM simulation (solid line represent theoretical predictions, and dashed line represents the FEM simulation results)

5. Conclusion

This paper aims at low-frequency, broadband and hybrid noise control in a ventilation ductwork system. The transverse HR array consisting of several tuned HRs mounted on the same cross-sectional area of a duct can provide several resonance peaks. However, the transverse HR array is still effective at its resonance frequencies with relative narrow bands. An array of transverse HRs array distributed periodically on the duct is therefore proposed to be the multiple HR arrays system. By taking the advantage of the coupling effects of Bragg reflection and resonances of the transverse HR array, the multiple HR arrays system could provide broader noise attenuation bands at designed resonance frequencies. The acoustic performance of the multiple HR arrays system is analyzed theoretically and numerically. In light of the interest of low frequencies in ventilation ductwork system, the frequency range considered in this paper is well below the cutoff frequency of the duct. It is therefore that only planar wave is considered in the duct. The transfer matrix method and the Bragg theory are developed to conduct the investigation. By introducing the periodicity, the multiple HR array system can provide much broader noise attenuation bands at the designed resonance frequencies due to the coupling effects of the Bragg reflection and HRs' resonances. It should be noted that the resonance wavelengths of the transvers HR array and the periodic distance have the relation of for broader noise attenuation bands at each resonance frequencies simultaneously. The theoretical predictions show good agreement with the three-dimensional FEM simulation results. The present study provides a practical way in low-frequency, broadband and hybrid noise control application of a ventilation ductwork system and the proposed multiple HR arrays system can be extended to other research areas in respect of HR.

Acknowledgements

This research did not receive any specific grant from funding agencies in the public, commercial, or not-for-profit sectors.

References

[1] Afram, A.; Janabi-Sharifi, F. Review of modeling method for HVAC systems. Appl Therm Eng 2014, 67(1-2), 507-519.

[2] Mak, C.M.; Wang, Z. Recent advances in building acoustics: An overview of prediction methods and their applications. Build Environ 2015, 91, 118-126.

[3] Cai, C.; Mak, C.M. Generalized flow-generated noise prediction method for multiple elements in air ducts. Appl Acoust 2018, 135, 136-141.

[4] Fry, A. Noise Control in Building Services, 1st ed.; Pergamon Press: Oxford, UK, 1987.

[5] Klepeis, N.E.; Nelson, W.C.; Ott, W.R.; Robinson, J.P.; Tsang, A.M.; Switzer, P.; Engelmann, W.H. The National Human Activity Pattern Survey (NHAPS): a resource for assessing exposure to environmental pollutants. J Expo Anal Environ Epidemiol 2001,11(3), 231–252.

[6] Goelzer, B.; Hansen, C.H.; Sehrndt, G. Occupational Exposure to Noise: Evaluation, Prevention and Control; World Health Organisation: Geneva, Switzerland, 2001.

[7] Leder, S.; Newsham, G.R.; Veitch, J.A.; Mancini, S.; Charles, K.E. Effects of office environment on employee satisfaction: a new analysis. Build Res Inf 2016, 44(1), 34-50.

[8] Miedema, H.M. Relationship between exposure to multiple noise sources and noise annoyance. J Acoust Soc Am 2004, 116, 949-957.

[9] Tzivian, L.; Winkler, A.; Dlugaj, M.; Schikowski, T.; Vossoughi, M.; Fuks, K.; Weinmayr, G.; Hoffmann, B. Effect of long-term outdoor air pollution and noise on cognitive and psychological functions in adults. Int J Hyg Environ Health 2015, 218, 1–11.

[10] Babisch, W.; Ising, H.; Gallacher, J.E.J. Health status as a potential effect modifier of the relation between noise annoyance and incidence of ischaemic heart disease. Occup Environ Med 2003, 60, 739-745.

[11] Ma, K.W.; Wong, M.H.; Mak, C.M. Dental environmental noise evaluation and health risk model construction to dental professionals. Int J Env Res Pub He 2017, 14(9), 1084.

[12] Axelsson, A.; Prasher, D. Tinnitus induced by occupational and leisure noise. Noise Health 2000, 2, 47.

[13] Yoshida, T.; Osada, Y.; Kawaguchi, T.; Hoshiyama, Y.; Yoshida, K.; Yamamoto, K. Effects of road traffic noise on inhabitants of Tokyo. J Sound Vib 1997, 205, 517–522.

[14] Evans, G.W.; Lercher, P.; Meis, M.; Ising, H.; Kolfer, W.W. Community noise exposure and stress in children. J Acoust Soc Am 2001, 109, 1023-1027.

[15] Namba, S.; Kuwano, S.; Okamoto, T. Sleep disturbance caused by meaningful sounds and effect of background noise. J Vib Acoust 2004, 277, 445-452.

[16] Hansen, C.H.; Snyder, S.D. Active Control of Noise and Vibration. E&FN Spon: London, UK, 1997.

[17] Chen, K.; Paurobally, R.; Pan, J.; Qiu, X.J. Improving active control of fan noise with automatic spectral reshaping for reference signal. Appl Acoust 2015, 87, 142-152.

[18] Peat, K.S.; Rathi, K.L. A finite element analysis of the convected acoustic wave motion in dissipative silencers. J Sound Vib 1995, 184, 529-545.

[19] Ingard, U. On the theory and design of acoustic resonators. J Acoust Sco Am 1953, 25, 1037-1061.

[20] Cai, C.; Mak, C.M. Noise attenuation capacity of a Helmholtz resonator. Adv Eng Softw 2018, 116, 60-66.

[21] Wang, X.N.; Choy, Y.S.; Cheng, L. Hybrid noise control in a duct using a light micro-perforated plate. J Acoust Soc Am 2012, 132(6), 3778-3787.

[22] Munjal, M.L. Acoustic of ducts and mufflers. 1st ed.; John Wiley & Sons: New York, USA, 1987.

[23] Cai, C.; Mak, C.M.; Shi, X. An extended neck versus a spiral neck of the Helmholtz resonator. Appl Acoust 2017, 115, 74-80.

[24] Xu, M.B.; Selamet, A.; Kim, H. Dual Helmholtz resonator. Appl Acoust 2010, 71, 822-829.

[25] Griffin, S.; Lane, S.A.; Huybrechts, S. Coupled Helmholtz resonators for acoustic attenuation. J Vib Acoust 2001, 123, 11-17.

[26] Park, S.H. Acoustic properties of micro-perforated panel absorbers backed by Helmholtz resonators for the improvement of low-frequency sound absorption. J Sound Vib 2013, 332, 4895-4911.

[27] Seo, S.H.; Kim, Y.H. Silencer design by using array resonators for low-frequency band noise reduction. J Acoust Soc Am 2005, 118(4), 2332-2338.

[28] Wu, D.; Zhang, N. The improvement on noise attenuation performance of a duct-resonator system. J Asian Archit Build 2017, 16(3), 669-674.

[29] Tang, S.K. Narrow side-branch arrays for low frequency duct noise control. J Acoust Soc Am 2012, 135, 3086-3097

[30] Bradley, C.E. Time harmonic acoustic Bloch wave propagation in periodic waveguides. Part I. Theory. J Acoust Soc Am 1994, 96, 1844-1853.

[31] Bradley, C.E. Time harmonic acoustic Bloch wave propagation in periodic waveguides. Part II. Experiment. J Acoust Soc Am 1994, 96, 1854-1862.

[32] Sugimoto, N.; Horioka, T. Dispersion characteristics of sound waves in a tunnel with an array of Helmholtz resonators. J Acoust Soc Am 1995, 97(3), 1446-1459.

[33] Cai, C.; Mak, C.M. Noise control zone for a periodic ducted Helmholtz resonator system. J Acoust Soc Am 2016, 140(6), EL471-EL477.

[34] Ji, Z.; Sha, J. Four-pole parameters of a duct with low Mach number flow. J Acoust Soc Am 1995, 98(5), 2848-2850.

Figure captions

Figure 1. A single side-branch Helmholtz resonator

Figure 2. A transverse HR array consisting of four different HRs (a) side view, (b) front view

Figure 3. Multiple Helmholtz resonator arrays installed on the duct

Figure 4. Configuration of transverse HR array consisting of four different HRs

Figure 5. Comparison of the transverse HR array and individual HRs

Figure 6. Comparison of theoretical predictions and the FEM simulation results (solid lines represent theoretical predictions, and dashed crosses represent the FEM simulation results)

Figure 7. Configuration of the multiple HR arrays system

Figure 8. Comparison of the side-branch transverse HR array and the transverse HR array as a periodic portion of the multiple HR array system

Figure 9. Comparison of theoretical predictions and the FEM simulation (solid line represent theoretical predictions, and dashed line represents the FEM simulation results)